

# Electrodeposition of platinum nanoparticles on highly oriented pyrolytic graphite

## Part II: Morphological characterization by atomic force microscopy

Guojin Lu<sup>a</sup>, Giovanni Zangari<sup>b,\*</sup>

<sup>a</sup> Department of Metallurgical and Materials Engineering, The University of Alabama, Tuscaloosa, AL 35487, USA

<sup>b</sup> Department of Materials Science and Engineering and Center for Electrochemical Science and Engineering, University of Virginia, Charlottesville, VA 22904, USA

Received 11 March 2005; received in revised form 26 July 2005; accepted 26 July 2005

Available online 2 September 2005

### Abstract

Platinum nanoparticles were electrochemically deposited onto highly oriented pyrolytic graphite (HOPG) from  $\text{H}_2\text{PtCl}_6$  solutions and observed by tapping mode atomic force microscopy. Spontaneous Pt deposition, which resulted in a wide particle size distribution, would occur on HOPG at open-circuit potential but could be suppressed by using anodic bias of the substrate before and after deposition. Nanoparticles with a narrow size distribution could be obtained when spontaneous reduction was avoided. Pt nucleated both at step edges and on terraces, with a preference for the former. The density of Pt nanoparticles on HOPG was  $10^9$ – $10^{10}$   $\text{cm}^{-2}$ . Increasing the deposition overpotential or adding HCl as supporting electrolyte resulted in more uniform particles and less aggregation. These findings confirm previous results obtained by our group using only electrochemical methods [G. Lu, G. Zangari, J. Phys. Chem. B 109 (2005) 7998].

© 2005 Elsevier Ltd. All rights reserved.

**Keywords:** Electrodeposition; Pt; AFM; HOPG; Nanoparticles

### 1. Introduction

Platinum nanoparticles with narrow size distribution dispersed onto smooth, non-catalytic surfaces are of interest as model systems for the investigation of particle shape and size dependence of the catalytic activity of platinum (Pt) towards reactions of interest in fuel cell systems. Electrodeposition on substrates with low surface energy, such as highly oriented pyrolytic graphite (HOPG) usually yields Volmer–Weber growth, i.e., a three-dimensional (3D) island growth mode, leading to nanoparticle formation and favoring the synthesis of well dispersed, uniform Pt nanoparticles [1].

In the first part of this series [2], we presented an electrochemical characterization of the reduction process of Pt onto HOPG, from dilute solutions of chloroplatinic acid

$\text{H}_2\text{PtCl}_6$ . We found that potentiostatic transients for Pt reduction mostly follow the behavior predicted for instantaneous 3D nucleation, and that the addition of HCl as supporting electrolyte strongly polarizes the reduction process and improves the instantaneous character of the deposition process. No *direct* evidence of instantaneous nucleation can however be obtained by electrochemical techniques.

Direct observation of nanoparticle formation onto HOPG is facilitated by the atomic smoothness of HOPG substrates, and it has indeed been reported both by Penner's group [3,4] and by others [5–10]. Penner et al. [1] in particular claim that the observation of nanoparticles on HOPG by STM (scanning tunneling microscopy) or contact AFM (atomic force microscopy) is misleading, since most nanoparticles are weakly bound to the substrate and would be swept away by the tip; only the particles grown at defects could in fact be observed under those conditions. Their group consequently chose to use non-contact AFM to observe nanoparticle

\* Corresponding author.

E-mail address: [gz3e@virginia.edu](mailto:gz3e@virginia.edu) (G. Zangari).

morphology. In this work, we choose to use tapping mode AFM, and we are able to observe the growth of particles both at defects and onto terraces.

In this paper, we present a systematic analysis of the morphology of nanoparticles electrodeposited onto HOPG using  $\text{H}_2\text{PtCl}_6$ -based electrolytes with a variable concentration of HCl as a supporting electrolyte. Our objective is to verify the nucleation and growth behavior deduced by electrochemical methods and discussed in Ref. [2], and to use these data to further optimize the preparation conditions for the production of Pt nanoparticles with narrow size distribution.

## 2. Experimental

Pt electrodeposition was carried out from 1 mM  $\text{H}_2\text{PtCl}_6$  solutions onto HOPG (10 mm  $\times$  10 mm  $\times$  1 mm, grade 2,

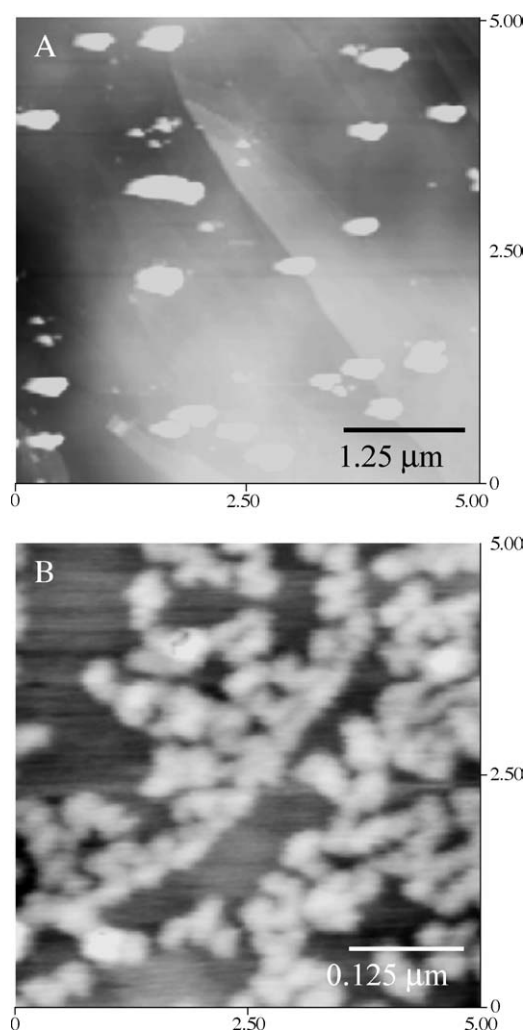


Fig. 1. (A) AFM image (5  $\mu\text{m} \times 5 \mu\text{m}$ , height scale 50 nm) of a HOPG surface after immersion in 1 mM  $\text{H}_2\text{PtCl}_6$  for 1 min at open circuit potential. The average height of the metal islands is about 15 nm. (B) AFM image (0.5  $\mu\text{m} \times 0.5 \mu\text{m}$ , height scale 2 nm) of Pt electrodeposits on untreated HOPG from 1 mM  $\text{H}_2\text{PtCl}_6$  at  $-0.1 \text{ V}$  for 10 ms. Average particle height is about 1 nm.

with an average terrace distance of about 500 nm) supplied by Structure Probe Inc. [11]. In some cases, 0.1–0.2 M HCl was added to the solutions as supporting electrolyte to tailor the nucleation and growth behavior [2]. The surfaces were prepared by cleaving the HOPG substrates and detaching a small number of graphitic planes using an adhesive tape, just prior to each experiment. The fluctuation in the number of defects of the new graphite surface exposed during cleavage is about 10–20% [3]. The deposition mode was potentiostatic. One short potential pulse from the open-circuit potential (about 0.55 V) to a value in the range 0 to  $-0.2 \text{ V}$  was applied for 1 ms to 1 s to control particle size. Here and in the following the potentials are referred to the Standard Calomel Electrode (SCE,  $V_{\text{SCE}} = 0.2415 \text{ V}_{\text{SHE}}$ ). The electrolyte was never stirred during the experiments. The electrochemical setup and other experimental details are described elsewhere [2].

Before each electrodeposition experiment, the HOPG substrate was immersed in the platinum plating electrolyte at a potential of 0.8 V for 2 min, to avoid electroless Pt deposition [4]. After application of the deposition pulse, the electrode potential was returned to 0.8 V for 2 s. Following deposition, the electrodes were removed immediately from

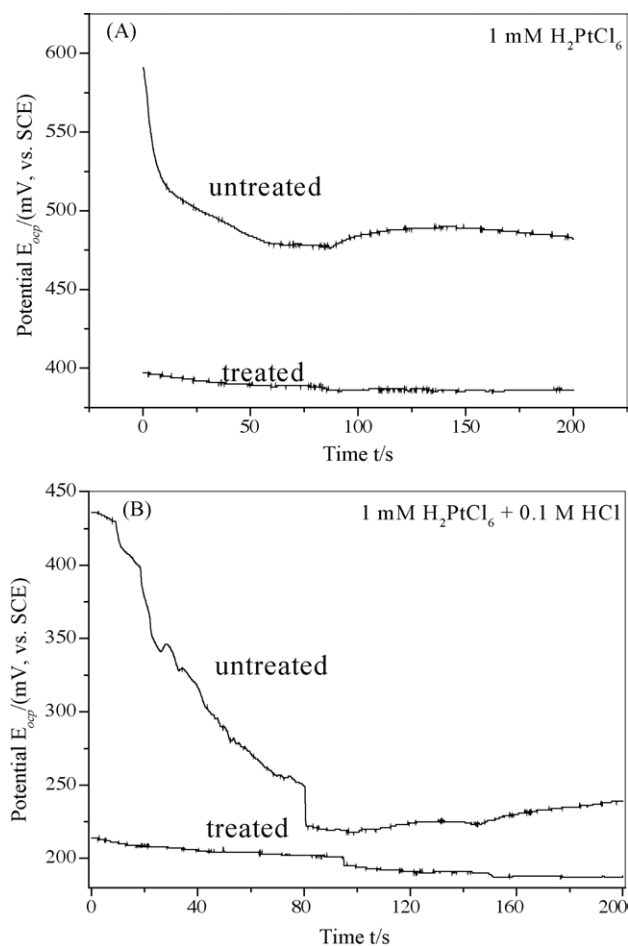


Fig. 2. Time evolution of the open circuit potential  $E_{\text{ocp}}$  of freshly cleaved HOPG, untreated or anodically biased as discussed in the text, immersed in (A) 1 mM  $\text{H}_2\text{PtCl}_6$  and (B) 1 mM  $\text{H}_2\text{PtCl}_6 + 0.1 \text{ M HCl}$ .

the electrolyte, rinsed thoroughly with deionized water, and then dried in air. The samples were stored in a desiccator and characterized shortly after their preparation.

The surface topography of the samples was imaged by using a Digital Instruments Nanoscope III AFM in air. All experiments were carried out with Ultrasharp™ noncontact silicon cantilevers of the 12 series–NSC12 tips, and with the AFM operating in the tapping mode with a tapping force of about  $10^{-12}$  N. Images of nanoparticle arrays with larger particle size were also obtained by scanning electron microscopy (Philips XL30 SEM) without any previous sample preparation. The presence of Pt on HOPG was independently ascertained by X-ray photoelectron spectroscopy (XPS), using a Kratos Axis165 electron spectrometer system.

Transmission electron microscopy (TEM) images and selected diffraction patterns of the Pt nanoparticles were obtained with a Hitachi H-8000 TEM instrument with an accelerating voltage of 200 KV. Samples for TEM analysis were prepared by first detaching and dispersing the weakly adsorbed Pt particles onto HOPG in isopropanol by ultrasonication. The particles in suspension were successively collected by pouring the suspension on a 3 mm diameter carbon-coated gold grid. The particle-supporting grid was air-dried before introduction and observation in the TEM.

### 3. Results and discussion

#### 3.1. Spontaneous Pt deposition

Pt reduction from chloride electrolytes is known to occur spontaneously at open circuit on defect sites of HOPG surfaces [4,12,13]. The thermodynamic driving force for this process is related to the presence of incompletely oxidized functionalities at terraces and kink sites [4]. We observed spontaneous reduction and agglomeration of Pt upon immersion of an as-cleaved HOPG substrate in a Pt chloride solution (Fig. 1A). After one minute of immersion the reduced Pt agglomerated into micron-sized islands, due to Ostwald ripening. The height of the particle islands was about 15 nm. At variance with Ref. [4], no preferential island growth at edge sites was observed. Spontaneous reduction occurred also while electrochemical reduction of Pt was performed; this resulted in strong aggregation and dendritic growth of the Pt islands, as shown in Fig. 1B (average particle height in this image is about 1 nm). In order to grow nano-sized Pt particles with uniform size it is thus necessary to inhibit this spontaneous reduction process.

Methods to avoid spontaneous Pt reduction include the chemical modification of HOPG with a self-assembled monolayer [13] or the electrochemical modification of the HOPG

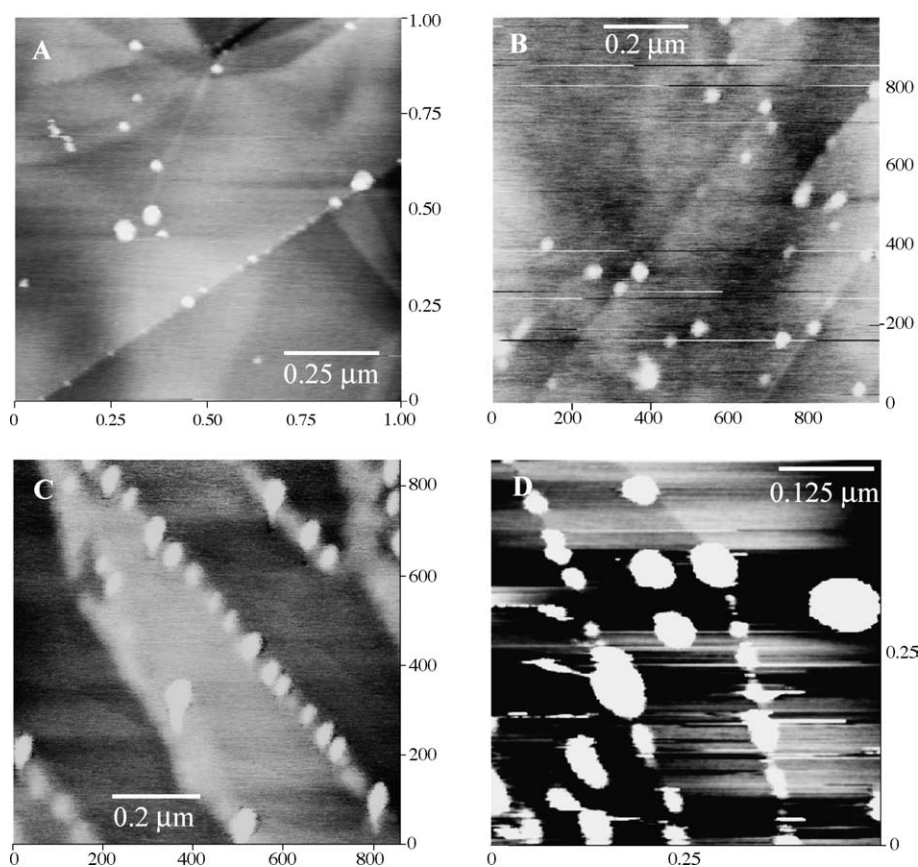


Fig. 3. AFM images of Pt electrodeposits on HOPG from 1 mM  $\text{H}_2\text{PtCl}_6$  at  $-0.1$  V for (A) 1 ms ( $1 \mu\text{m} \times 1 \mu\text{m}$ , height scale 2 nm); (B) 3 ms ( $0.98 \mu\text{m} \times 0.98 \mu\text{m}$ , height scale 2 nm); (C) 10 ms ( $0.862 \mu\text{m} \times 0.862 \mu\text{m}$ , height scale 3 nm) and (D) 100 ms ( $0.5 \mu\text{m} \times 0.5 \mu\text{m}$ , height scale 3 nm).

surface by anodic polarization [4,12]. In the present study, the latter method was used: a potential of 0.8 V was applied to the substrate in the electroplating solution before (for 2 min) and after (for 2 s) application of the reduction pulse. The anodic pretreatment has an important effect on the HOPG surface state, as monitored by the temporal evolution of the open circuit potential OCP in the electrodeposition solution shown in Fig. 2. While the OCP of the untreated electrode decreases slowly with time, the OCP of the treated substrate is stable at a lower value. The OCP of the untreated electrode in 1 mM  $\text{H}_2\text{PtCl}_6$  (Fig. 2A) is near to the redox potentials of the  $\text{PtCl}_6^{2-}/\text{Pt}$  and  $\text{PtCl}_4^{2-}/\text{Pt}$  couples (0.503 and 0.517  $V_{\text{SCE}}$ , respectively), indicating that one of these processes tends to approach equilibrium and that Pt reduction might have occurred during the OCP transient. The lower and stable potential observed on the treated substrate on the other hand indicates that the above redox reactions are probably not occurring. The OCPs are lower in the HCl-supported solution (Fig. 2B) but the trends and time scale are similar, suggesting that the only difference in the latter electrolyte might be a stronger complexation of Pt by chlorides.

Inhibition of spontaneous reduction was demonstrated by subjecting a HOPG surface to a 2 min anodic treatment, then leaving the sample in the electrodeposition solution at OCP for an additional 2 min. Only few Pt particles were observed by AFM in this case (not shown), with a much smaller height (<10 nm) and size (<100 nm), indicating that the spontaneous deposition of Pt was effectively suppressed by the anodic pretreatment.

### 3.2. Electrochemical deposition of Pt

In part I of this series [2], electrochemical methods were used to identify a transition of the Pt nucleation mode from progressive to instantaneous with increasing overpotential. This transition occurred between 0 and  $-0.2$  V in unsupported 1 mM  $\text{H}_2\text{PtCl}_6$ . The instantaneous character of the nucleation process became even more evident after addition of chloride anions to the electrolyte. In this section, we report on the shape, size and dispersion of electrodeposited Pt nanoparticles as a function of deposition potential and of the electrolyte composition.

Fig. 3 shows AFM images of Pt nanoparticles grown from unsupported 1 mM  $\text{H}_2\text{PtCl}_6$  at  $-0.1$  V for various deposition times, from 1 to 100 ms. Evidence that the approximately circular features seen in the AFM images are Pt nanoparticles was independently obtained by collecting XPS spectra on these samples.

Pt nanoparticles grow both at step edges and on terraces; however, preference for nucleation at step edges is apparent; this is commonly observed for electrodeposition on HOPG [3,4,8,9,14–16]. It was claimed by others that defects on terraces, such as surface vacancies can also act as nucleation centers, although they may not be visible by AFM at the resolution we employed [17,18]. The nanoparticles are for the

most part well separated and, particularly at short deposition times, present a relatively uniform size.

AFM provides accurate measurements of particle heights, but the apparent nanoparticle diameters are exaggerated due to convolution of the particle shape with the silicon tip, which has a nominal radius of curvature of the order of 10 nm [3]. The error introduced by this convolution effect is important, particularly for the smallest particles seen in Fig. 3A and B, which appear larger than they actually are. In order to obtain a better estimate of particle size in these instances, deconvolution of the AFM images is needed. When the tip radius  $R$  (in this case, about 10 nm) is comparable to or larger than the typical size  $r$  of the particle of interest, i.e.,  $R \geq r$ , the relationship between the apparent particle size  $r_c$  seen by the AFM and its real size is approximately [19]:

$$r_c = 2\sqrt{Rr} \Rightarrow r = \frac{r_c^2}{4R} \quad (1)$$

It should be stressed that this determination of particle size is approximate, since 10 nm is a nominal tip radius of curvature; this value can vary and further change during the measurement.

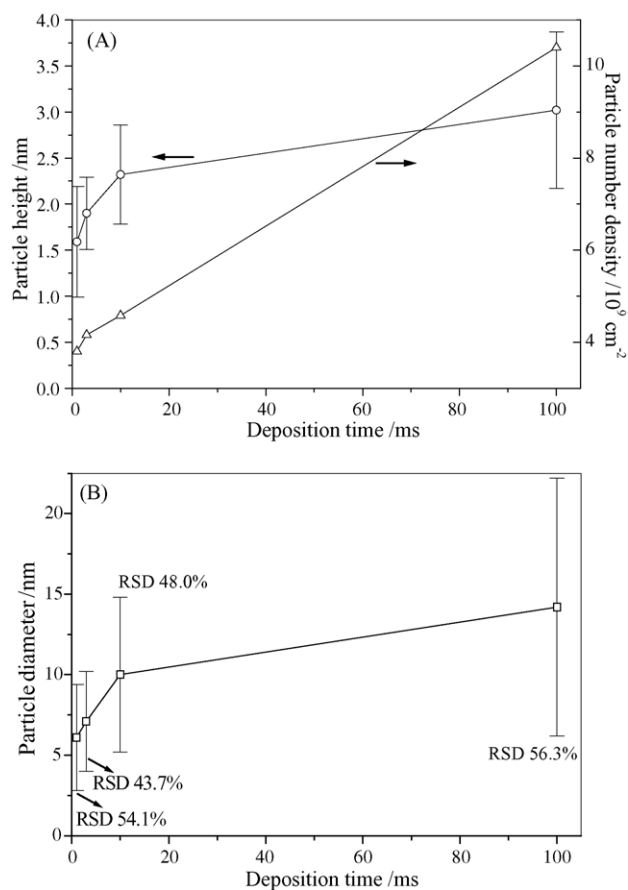


Fig. 4. The variation of average particle height and particle number density (A) and average particle diameter (B) with deposition time based on the statistical analysis of data similar to those presented in Fig. 3.

The distribution of particle heights, particle number density, and real particle size (calculated from Eq. (1)) versus deposition time were determined through a statistical analysis of images similar to those of Fig. 3. Each distribution was determined using two nominally identical samples grown in different deposition experiments and images obtained at three locations for each sample. Average values are reported in Fig. 4A (particle height and particle number density) and B (calculated particle diameter). Relative standard deviations (R.S.D.: standard deviation/mean value) of the height and diameter distributions are shown as error bars in the same plots.

The average particle height varies from from 1.5 to 3 nm, while the average apparent particle diameter varies from about 6 to 14 nm. The diameter/height ratio for these particles is thus of the order of 4, suggesting that the particles tend to be approximate spherical caps. Some larger particles have an apparent diameter/height ratio (without deconvolution) of the order of 25 or more and are apparently disk-shaped.

As indicated by the R.S.D. values in Fig. 4, both the height and diameter distributions broaden with increasing deposition times and reach relatively high values. The number density of particles estimated from the AFM data is between  $10^9$  and  $10^{10} \text{ cm}^{-2}$  (note that the scales for the images in

Fig. 3 are different), and increases by three times between 1 and 100 ms deposition time. These data indicate that a progressive nucleation mode occurs at  $-0.1 \text{ V}$ , in agreement with our previous finding [2].

The diffusion limited growth of non-interacting particles should yield an increasingly narrower size distribution [1]. The observed broadening of the height and diameter distributions is opposite to this trend and can be explained as the result of interactions between the ion-depleted electrolyte regions around the nuclei, which tend to change the growth rate of each particle. Such effect will be most pronounced at step edges, where particles nucleate preferentially.

Pt nanoparticles were deposited onto HOPG from 1 mM  $\text{H}_2\text{PtCl}_6$  also at potentials varying between 0 and  $-0.2 \text{ V}$ . Narrower height and diameter distributions were observed with decreasing deposition potential (increasing overpotential), in agreement with the observed increase of the instantaneous character of the nucleation process at more cathodic potentials [2].

Upon addition of HCl to the electrolyte, Pt nanoparticles electrodeposited at  $-0.1 \text{ V}$  exhibit a higher number density and a narrower size distribution, as shown in Fig. 5 for deposition times varying between 1 and 500 ms. Fig. 6 shows the change in average particle height, particle number density

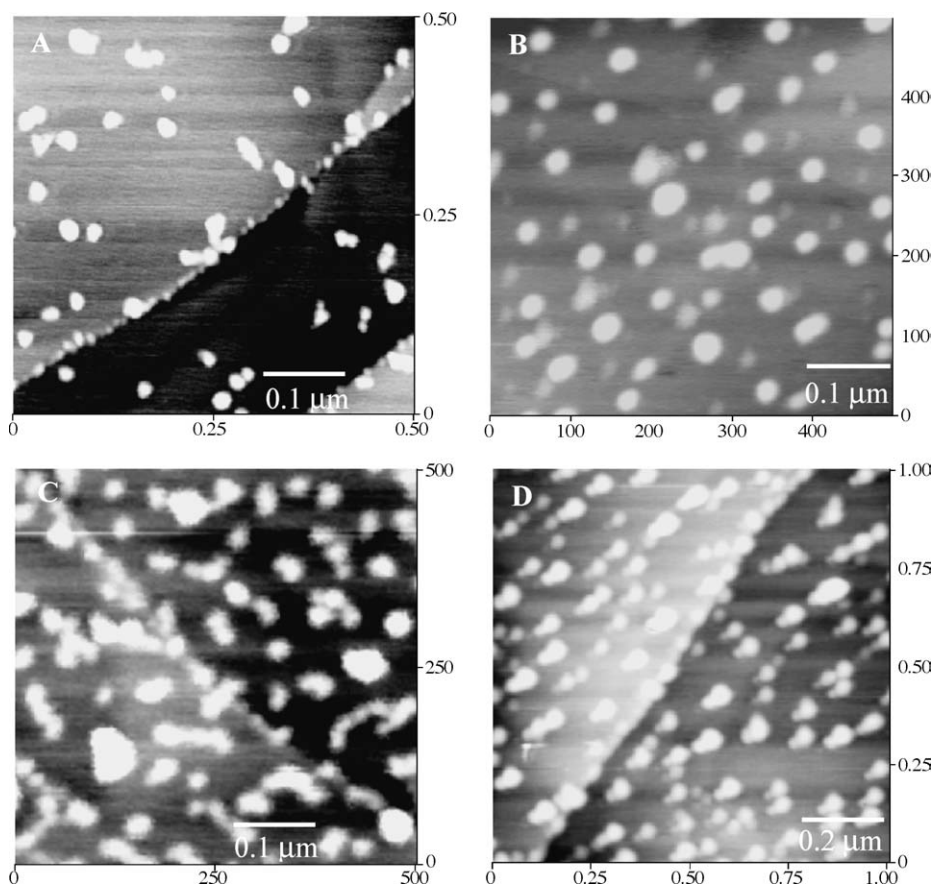


Fig. 5. AFM images of Pt electrodeposits on HOPG from 1 mM  $\text{H}_2\text{PtCl}_6$  + 0.1 M HCl at  $-0.1 \text{ V}$ , for (A) 1 ms ( $0.5 \mu\text{m} \times 0.5 \mu\text{m}$ , height scale 2 nm); (B) 10 ms ( $0.5 \mu\text{m} \times 0.5 \mu\text{m}$ , height scale 2 nm); (C) 100 ms ( $0.5 \mu\text{m} \times 0.5 \mu\text{m}$ , height scale 3 nm) and (D) 500 ms ( $1.006 \mu\text{m} \times 1.006 \mu\text{m}$ , height scale 5 nm).

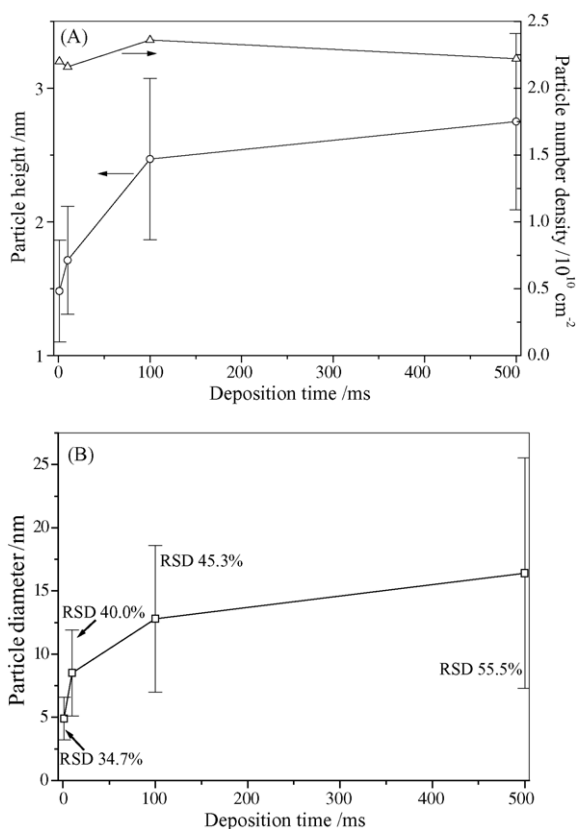


Fig. 6. The variation of average particle height and particle number density (A) and average particle diameter (B) with deposition time as determined from a statistical analysis of data similar to those presented in Fig. 5.

and average diameter with deposition time based on a statistical analysis of images similar to those of Fig. 5. Again, each analysis was performed using two nominally identical samples and three different locations on each sample. The particle heights and diameters are smaller and their distribution narrower (see the R.S.D. values in Fig. 6) than in the previous case, when no HCl was added. This is probably due both to the inhibition of Pt electroreduction, which increases the overvoltage for deposition, and to the increase in the instantaneous character of the nucleation process induced by chloride adsorption, as described in Ref. [2]. The Pt nanoparticles are better separated and have a lower tendency to aggregate when electrodeposited from  $\text{Cl}^-$ -containing solutions. This may occur because chloride anions adsorb on Pt particles, preventing coalescence of neighboring particles due to the electrostatic repulsion between adsorbed  $\text{Cl}^-$  layers [10]. Particle number density is also higher upon addition of  $\text{Cl}^-$ . Possible reasons include the higher nucleation density due to the increase of the deposition overpotential [2] and again the prevention of aggregation by chloride adsorption on Pt particles. The particle number density in this case is approximately constant up to 500 ms deposition, indicating that no new Pt nuclei are formed and that the nucleation process is now truly instantaneous. SEM images of Pt deposits grown for times as long as 10 min from supported electrolytes were also collected, showing very uniform and homogeneously distributed Pt particles, with an average particle size of about 150 nm. Instantaneous nucleation from supported solutions is even more evident when the  $\text{Cl}^-$  concentration is increased to 0.2 M.

AFM data indicate that Pt nanoparticles of larger size have a lower height/diameter ratio, and consequently smaller

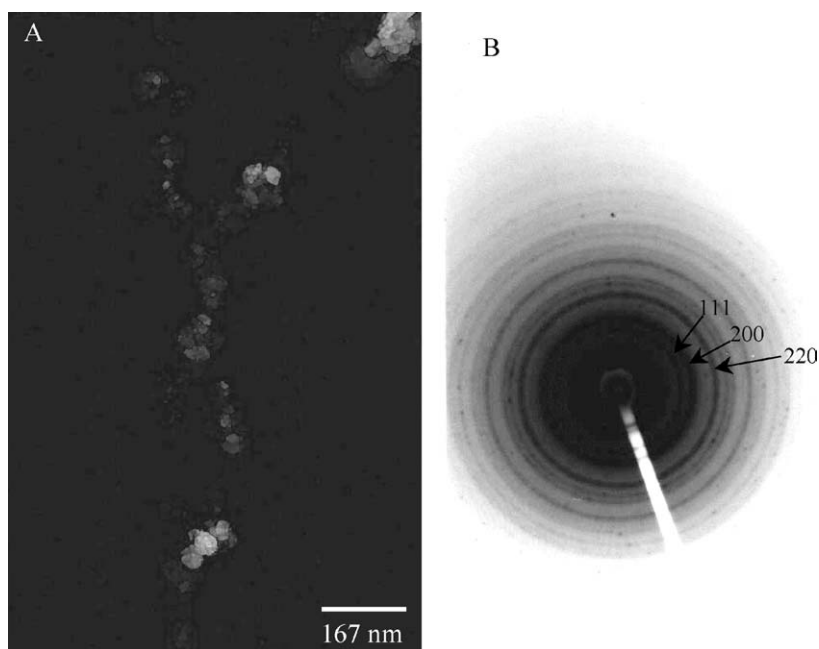


Fig. 7. (A) Transmission electron microscope image of platinum nanoparticles deposited from 1 mM  $\text{H}_2\text{PtCl}_6$  + 0.1 M HCl at  $-0.1$  V for 2 s. (B) Selected area electron diffraction pattern of the image in (A). The main diffraction rings are indicated by arrows.

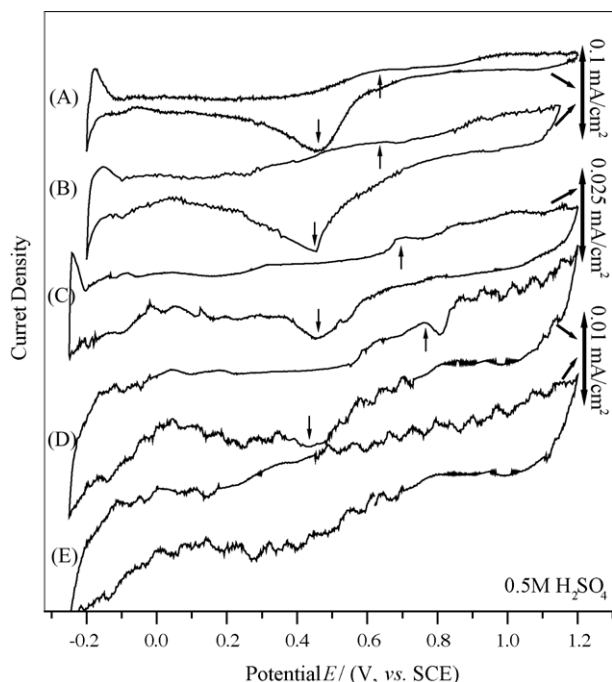


Fig. 8. Typical cyclic voltammograms obtained at a scan rate of 20 mV/s in 0.5 M  $\text{H}_2\text{SO}_4$  for bulk Pt sheet (A) and Pt electrodeposits onto HOPG from 1 mM  $\text{H}_2\text{PtCl}_6$  + 0.1 M HCl at  $-0.1$  V grown for various deposition times (B) 600 s; (C) 1 s; (D) 1 ms and (E) freshly cleaved HOPG surface without Pt.

particles are approximately spherical while larger ones are more disk-like. Since we are interested in the morphological features of nanoparticles, TEM imaging of Pt nanoparticles separated from the substrate was performed to independently and directly verify the above statements. Fig. 7A shows a typical TEM image of Pt particles deposited on HOPG from a solution containing 1 mM  $\text{H}_2\text{PtCl}_6$  + 0.1 M HCl at  $-0.1$  V for 2 s. Particle size is around 20 nm. In addition, particle shape is approximately, but not strictly, spherical. Particle polygonization is possible but cannot be resolved at the magnification used. Electron diffraction (Fig. 7B) on these samples provides further evidence that the nanoparticles are metallic Pt. The radii of the first three diffraction rings in fact correspond to the atom-to-atom distances  $d = 0.227$ , 0.198 and 0.139 nm, which are very close to the handbook values of 0.2265 nm for the (1 1 1), 0.196 for the (2 2 0), and 0.139 for the (2 2 0) planes of bulk fcc platinum [20], respectively.

An initial characterization of the electrocatalytic properties of Pt nanoparticles was performed by collecting cyclic voltammograms of supported Pt nanoparticle electrodes immersed in 0.5 M  $\text{H}_2\text{SO}_4$ , as shown in Fig. 8. CVs for bulk Pt and for a bare HOPG surface are also shown for comparison. The CV of large Pt particles is similar to that of a polycrystalline platinum surface. In particular, it is possible to observe the hydrogen adsorption and desorption features as well as the platinum oxide formation and reduction waves. However, small Pt particles (smaller than 10 nm) do not exhibit CV peaks for hydrogen adsorption or desorption. This is perhaps

due to the small signal coming from small Pt particles in comparison with the spurious signal from the HOPG support [21]. Despite the noise, there seems to be a trend for smaller Pt particles to exhibit a larger irreversibility for Pt oxide formation and reduction, as indicated by the increasing potential gap between the oxidation and reduction waves with decreasing deposition time [4].

#### 4. Conclusions

Platinum nanoparticles have been grown on HOPG by electrodeposition from chloride-based electrolytes. Spontaneous Pt deposition at open circuit was avoided by anodic bias of the substrate before and after deposition. Approximately spherical nanoparticles with a narrow size distribution can be obtained from 1 mM  $\text{H}_2\text{PtCl}_6$  solution at relatively high overpotential. Pt particles nucleated both at step edges and on terraces, with a preference for the former. The number density of Pt particles on HOPG is in the range  $10^9$ – $10^{10}$   $\text{cm}^{-2}$ . Increasing the deposition overpotential or adding HCl (0.1–0.2 M) as supporting electrolyte resulted in a more uniform size distribution, higher particle number density and less aggregation. In addition, particle number density in the latter case was constant indicating strict instantaneous nucleation. These results confirm former findings obtained by electrochemical methods only [2]; in particular, it is verified that electrodeposition from HCl-supported electrolytes results in instantaneous nucleation and in the synthesis of Pt nanoparticle arrays with an increasingly narrow size distribution.

#### Acknowledgements

This work was financially supported by the United States Department of Energy (US DOE) EPSCoR Implementation, under Grant No.: DE-FG02-ER45867 and by Grant No. NSF-DMR 0093154.

Dr. Gary J. Mankey of the Department of Physics and MINT center, University of Alabama is gratefully acknowledged for insightful discussion and technical assistance. The use of MRSEC shared Facilities was supported under Grant No. NSF-DMR-9809423.

#### References

- [1] R.M. Penner, *J. Phys. Chem. B* 106 (2002) 3339.
- [2] G. Lu, G. Zangari, *J. Phys. Chem. B* 109 (2005) 7998.
- [3] J.V. Zoval, R.M. Stiger, P.R. Biernacki, R.M. Penner, *J. Phys. Chem.* 100 (1996) 837.
- [4] J.V. Zoval, J. Lee, S. Gorer, R.M. Penner, *J. Phys. Chem. B* 102 (1998) 1166.
- [5] F. Gloaguen, J.M. Leger, C. Lamy, A. Marmann, U. Stimming, R. Vogel, *Electrochim. Acta* 44 (1999) 1805.
- [6] Y. Gimeno, A. Hernandez Creus, S. Gonzalez, R.C. Salvarezza, A.J. Arvia, *Chem. Mater.* 13 (2001) 1857.

- [7] A.C. Hill, R.E. Patterson, J.P. Sefton, M.R. Columbia, *Langmuir* 15 (1999) 4005.
- [8] A.E. Alvarez, D.R. Salinas, *J. Electroanal. Chem.* 566 (2004) 393.
- [9] I. Lee, K.-Y. Chan, D.L. Phillips, *Ultramicroscopy* 75 (1998) 69.
- [10] I. Lee, K.-Y. Chan, D.L. Phillips, *Appl. Surf. Sci.* 136 (1998) 321.
- [11] [www.2spi.com](http://www.2spi.com).
- [12] P. Shen, N. Chi, K.-Y. Chan, D.L. Phillips, *Appl. Surf. Sci.* 172 (2001) 159.
- [13] S. Liu, Z. Tang, E. Wang, S. Dong, *Electrochem. Commun.* 2 (2000) 800.
- [14] E. Gomez, E. Gaus, F. Sanz, E. Valles, *J. Electroanal. Chem.* 465 (1999) 63.
- [15] D.R. Salinas, E.O. Cobo, S.G. Garcia, J.B. Bessone, *J. Electroanal. Chem.* 470 (1999) 120.
- [16] R.T. Potzschke, C.A. Gervasi, S. Vinzelberg, G. Staikov, W.J. Lorenz, *Electrochim. Acta* 40 (1995) 1469.
- [17] H.-F. Waibel, M. Kleinert, L.A. Kibler, D.M. Kolb, *Electrochim. Acta* 47 (2002) 1461.
- [18] M. Aktary, C.E. Lee, Y. Xing, S.H. Bergens, M.T. McDermott, *Langmuir* 16 (2000) 5837.
- [19] M. Rasa, B.W.M. Kuipers, A.P. Philipse, *J. Colloid Interface Sci.* 250 (2002) 303.
- [20] JCPDS international centre for diffraction data # 04-0802.
- [21] L.-C. Jiang, D. Pletcher, *J. Electroanal. Chem.* 149 (1983) 237.